14-3-3ζ IS AMPLIFIED, OVEREXPRESSED AND PROCESSES ONCOGENIC ACTIVITIES IN HEAD AND NECK SQUAMOUS CELL CARCINOMA

Mauting Lin[1], Carl D. Morrison[3], Susie Jones[2], Nehad Mohamed[2], Jason Bacher[2], and Christoph Plass[1,4]

[1]Department of Molecular Virology, Immunology and Medical Genetics, Division of Human Cancer Genetics and [2]Department of Pathology, The Ohio State University Medical Center, Columbus, Ohio, 43240; [3]Department of Pathology and Laboratory Medicine, Roswell Park Cancer Institute, Buffalo, New York, 14263; [4]German Cancer Research Center, Division C010, Toxicology and Cancer Risk Factors, Im Neuenheimer Feld 280, 69120 Heidelberg, Germany

Running Title: 14-3-3ζ overrepresentation in HNSCC

Keywords: HNSCC, amplification, 14-3-3ζ

To whom correspondences should be addressed:

Christoph Plass
German Cancer Research Center
Division C010, Toxicology and Cancer Risk Factors
Im Neuenheimer Feld 280
69120 Heidelberg, Germany
Phone: +49-6221-42-3300
Fax: +49-6331-42-3359
E-mail: c.plass@dkfz.de

Abstract

Gene amplification, a common mechanism for oncogene activation in cancers, has been used in the discovery of novel oncogenes. DNA amplification is frequently observed in head and neck squamous cell carcinomas (HNSCCs) where numerous amplification events and potential oncogenes have already been reported. Recently, we applied restriction landmark genome scanning (RLGS) to study gene amplifications in HNSCC and located novel amplified and uncharacterized regions in primary tumor samples. DNA amplification on 8q22.3, the location of 14-3-3ζ (YWHAZ, KCIP-1) is found in 30-40% HNSCC cases. Data obtained from fluorescent *in-situ* hybridization (FISH) and immunohistochemistry on HNSCC tissue microarrays confirmed frequent low-level 14-3-3ζ copy number gains and protein overexpression. 14-3-3ζ mRNA was frequently upregulated in patients' tumor tissues. Furthermore, 14-3-3ζ RNAi significantly suppressed the growth rate of HNSCC cell lines, and overexpression of 14-3-3ζ in HaCaT immortalized human skin keratinocytes promotes its growth, as well as morphological changes. Reduced 14-3-3ζ levels increased the G1/G0-phase proportion, decreased the S-phase proportion and the rate of DNA synthesis. Based on this evidence, we suggest that 14-3-3ζ is a candidate proto-oncogene and deserves further investigations into its role in HNSCC carcinogenesis.

Introduction

Gain of DNA copy numbers, or DNA amplification, is a common genetic alteration found in many cancers (Schwab & Amler, 1990). Subchromosomal DNA amplification results in extra copies of specific regions, potentially containing growth-promoting oncogenes. DNA amplification results in overexpression of the target genes located in the amplified regions, and thus confers a growth advantage (Schwab, 1999). Overexpression of oncogenes results in neoplastic transformation and confers an advantage either by providing resistance to apoptotic stimuli (Lyons & Clarke, 1997) or by promoting accelerated cell growth (Neve et al., 2001). Amplification and overexpression of oncogenes is an early event in carcinogenesis (Schwab & Amler, 1990) and thus can be used as a diagnostic marker for early detection of tumor cells or to predict outcome of a clinical therapy. Furthermore, activated oncogenes provide potential targets for cancer therapies as shown for c-Myc in oesophageal cancer (Bitzer et al., 2003) or EGFR in lung cancer (Gallegos Ruiz et al., 2007).

In an earlier study we used restriction landmark genomic scanning (RLGS) to locate novel and known amplified chromosomal regions (Lin et al., 2006). In these amplified regions, we found oncogenes which are well-connected to HNSCC carcinogenesis, including the PI-3 kinase catalytic α subunit (PIK3CA) on chromosome 3q26.3, c-Myc (MYC) on 8q24.21 or cyclin D1 (CCND1) on 11q13.3. In addition, other novel and frequent amplicons on chromosome 3q29 and 8q22.3 were identified and confirmed. Each of these alterations was observed in approximately 30-40% HNSCC cases and considered a frequent alteration. Oncogenes in these regions have not yet been identified. Interestingly, RLGS fragment 2C13 on 8q22.3, identified as a frequently

amplified sequence is located in the 5' exon of tyrosine 3-monooxygenase/tryptophan 5-monooxygenase activation protein, zeta (YWHAZ), a 14-3-3 zeta isoform.

The 14-3-3 gene family was first discovered in 1967 during classification of cow brain proteins (Moore & Perez, 1967). Currently seven distinct isoforms (β, γ, ε, η, σ, τ and ζ) encoded by seven distinct genes have been identified in mammalian systems (Aitken et al., 1995). 14-3-3 family members are 28-33 kDa proteins which can homo- or heterodimerize (Jones et al., 1995). Dimerized 14-3-3 molecules bind to specific phosphor-serine/threonine (pS/-T)-containing motifs, two of which are RSXpSXP and RXXXpSXP (Rittinger et al., 1999; Yaffe et al., 1997). Many molecules regulating cell signaling (PKC, Raf-1, β-catenin) and apoptosis (Bad, Bax) are known that bind to 14-3-3 proteins (Braselmann & McCormick, 1995; Nomura et al., 2003; Robinson et al., 1994; Tian et al., 2004; Yang et al., 2001), which make them master-regulators of these regulators. Evidence for involvement in cancer comes from studies on 14-3-3σ, which is frequently hypermethylated and down-regulated in various types of cancers (Green, 2002; Muller et al., 2000; Richard et al., 2003) but overexpressed in others, possibly in response to cellular stress (Okada et al., 2006; Perathoner et al., 2005; Villaret et al., 2000). Its cooperation with several regulators to block cell cycle progression makes 14-3-3σ an ideal tumor-suppressor gene (Laronga et al., 2000; Lee & Lozano, 2006; Yang et al., 2003).

Previous reports showed overexpression of 14-3-3ζ in oral, stomach cancers and lung adenocarcinomas (Arora et al., 2005; Jang et al., 2004; Li et al., 2006; Neal, 2004; Ralhan et al., 2008) with the latter tumor type also showing gene amplification. In this work we demonstrated the overall

overrepresentations of 14-3-3ζ in DNA, mRNA and protein levels in HNSCC patients, followed by its capabilities to control cell growth when being negatively or positively manipulated. Furthermore, we examined its effects on the cell cycle and discussed how the activated gene could contribute to tumor progression.

Materials and Methods

HNSCC patient samples

Primary HNSCC derived from the nasal cavity, oral cavity, larynx and pharynx were obtained from the Cooperative Human Tissue Network. Surgery was performed on all patients at The Ohio State University. All normal specimens were harvested from morphologically normal appearing tissue located at least 3 cm distant from the tumor and were used as the normal control tissue for comparisons with the tumor. Quality control hematoxylin and eosin sections were performed for both normal and primary tumor and reviewed by a pathologist (CM). Samples were snap frozen in liquid nitrogen and stored at –80°C prior to DNA isolation. The study was performed under a protocol approved by the Institutional Review Board of The Ohio State University. The detailed protocols for genomic DNA preparation were described in our previous study (Lin et al., 2006).

RNA extraction, cDNA synthesis and semi-quantitative real-time RT-PCR

Total RNAs of an independent panel from additional 44 pairs of patients' normal and tumor tissues were extracted according to the standard TRIzol protocol of RNA extraction (Invitrogen, Carlsbad, CA). Following DNase I (Invitrogen) treatment to remove genomic DNA, 1-2μg of total RNA after was incubated with primers of 0.5μg oligo-deoxythymidine (dT) and 2μg random hexamers, and deoxynucleotide triphosphates (dNTPs) (10mM) for 5 min at 65°C in supplied RT-PCR buffer (Invitrogen). 50U of SuperScript II (Invitrogen) was added for 50 min at 42°C, followed by heat inactivation at 70°C for 15 min. Remaining RNA templates were removed by 37°C, 20-min RNase H incubation (Invitrogen). cDNAs are stored in -20°C.

14-3-3ζ and glycosylphosphatidylinositol (GPI, for internal control) cDNA levels were measured using SYBR Green I (BioRad, Hercules, CA) in a BioRad I-Cycler. Data were acquired in the format of cycle number crossing the software-generated threshold (Ct). The average of differences in Ct between 14-3-3ζ and GPI (ΔCt) from all normal tissues was defined as basal level (BL). Normalized 14-3-3ζ cDNA levels in tumors were calculated using the formula $1.9^{-(\Delta CtTumor-BL)}$. (1.9 is the amplification fold per cycle determined by calibrating experiments). We defined the normal 14-3-3ζ expression range as 0.5 to 2 folds of BL.

Construction of HNSCC tissue microarray (TMA)

The tissue microarray was constituted of 33 samples from previously studied samples (Lin et al., 2006). Triplicate 1-mm tissue cores from each of 48 formalin-fixed paraffin embedded donor blocks of HNSCC tumors and their normal counterparts were precisely arrayed into a new recipient paraffin block. Specimens for controls consisted of multiple cores of normal tissue from 10 different organs including heart, colon, kidney, adrenal, ovary, myometrium, brain, thyroid, lung, and prostate.

Fluorescent *in situ* hybridization (FISH) and immunohistochemical staining

FISH for 14-3-3ζ was done using the BAC clone RP11-302J23 (chr8: 102,004,801-102,195,725, UCSC Genome Bioinformatics, Mar 2006 release) which was verified by PCR to contain the 14-3-3ζ gene. FISH slides were prepared and scanned as previously described (Morrison et al., 2005). A ratio of the total number of 14-3-3ζ signals to the total number of CEP8 signals in at

least 60 interphase nuclei with no overlapping nuclei in the tumor cells was determined. Cells with no signals or with signals of only one color were disregarded. Tumor cells displaying at least two centromeric chromosome 8 signals and multiple 14-3-3ζ signals, with a 14-3-3ζ:CEP8 ratio of ≥2, were considered consistent with amplification of the 14-3-3ζ gene. Tumor cells displaying at least two centromeric chromosome 8 signals and an equal number of 14-3-3ζ signals, with a 14-3-3ζ:CEP8 ratio of less than 2, were considered consistent with no amplification of the 14-3-3ζ gene. Tumor cells displaying multiple CEP8 signals and an approximately equal number of 14-3-3ζ signals, with a somewhat random distribution of both, were considered polysomic chromosome 8.

Immunohistochemical staining was performed on formalin-fixed, paraffin-embedded TMA sections. Paraffin embedded tissue was cut at 4 microns and placed on positively charged slides. Slides with specimens were then placed in a 60°C oven for 1 hour, cooled, and deparaffinized and rehydrated through xylenes and graded ethanol solutions to water. All slides were quenched for 5 minutes in a 3% hydrogen peroxide solution in water to block for endogenous peroxidase. Slides were antigen retrieved in a solution of citrate buffer in a vegetable steamer. Slides were then placed on a Dako Autostainer, immunostaining system, for use with immunohistochemistry. Primary rabbit polyclonal anti-14-3-3ζ antibody clone C-16 (Santa Cruz Biotechnology, Santa Cruz, CA) was diluted 1:1500 and incubated for 60 minutes. Detection system used was a labeled polymer system, Envision Plus Dual Link (Dako code number K4061). Staining was visualized with DAB chromogen (Dako code number K3468). Slides were then counterstained in Richard Allen hematoxylin, dehydrated through graded ethanol solutions

and coverslipped.

Cell lines and culture

Four HNSCC cell lines (UMSCC-8, -9, -11B and -22B) and one immortalized human skin keratinocyte (HaCaT) were maintained and grown in Dulbecco's Modified Eagle's Medium (DMEM) with 10% Fetal Bovine Serum (FBS) and 1% streptomycin/penicillin (S/P) antibiotics.

RNAi transfection

Negative control (GGG-UAU-CGA-CGA-UUA-CAA-AUU-dTdT)) and 14-3-3ζ (AGU-UCU-UGA-UCC-CCA-AUG-C-dTdT) RNAi probes, previously published (Neal, 2004), were ordered through Qiagen (Valencia, CA). Lipofectamine 2000 transfection reagent (Invitrogen) was mixed with RNAi in a 1:1 ratio (v/v) at room temperature for 20 minutes. Cells were incubated with serum-free DMEM of 60nM negative control or 14-3-3ζ RNAi for 6 hours, then replaced with regular 10% FBS DMEM. The RNAi sequence of choice did not affect the levels of 14-3-3β and 14-3-3τ which have been tested by Neal's work.

Western blotting

Cells from 100-mm dishes were trypsinized, harvested, and lysed in lysis buffer containing 0.1% NP-40 and phosphatase inhibitor cocktails. 10μg of cell lysates were electrophoresed in 12% polyacrylamide gel, then transferred onto Amersham Hybond ECL nitrocellulose membrane (GE Healthcare Bio-Sciences, Piscataway, NJ). For standard Western protocol, the membrane was blocked with 3% non-fat milk at room temperature for 2 hours. After one

wash with TBS wash buffer (0.1% Tween-20), adequate primary antibodies were applied and incubated for 1 hour, following by two 15-min washes. Peroxidase-conjugated secondary antibodies were incubated with the membrane for 1 hour. Another two washes later we used Supersignal (Pierce Biotechnology, Rockford, IL) to detect signals developed on Blue Autoradiography Film (ISC BioExpress, Kaysville, UT). Antibody concentrations were as follows: rabbit anti-14-3-3ζ (Santa Cruz Biotechnology), 1:1000; mouse anti-α-tubulin (Calbiochem, San Diego, CA), 1:1000; mouse anti-HA tag clone 6E2 (Cell Signaling Technology, Danvers, MA), 1:1000; mouse anti-E-cadherin (Santa Cruz Biotechnology), 1:100; mouse anti-vimentin (Santa Cruz Biotechnology), 1:100; goat anti-rabbit & anti-mouse, HRP-conjugated (Biorad), 1:5000.

Cell growth curve assay

Twenty thousand HNSCC or HaCaT cells were seeded onto 6-well plates or 60-mm dishes depending on the proliferating potential of individual cell lines. After treatment, cells were trypsinized and counted by cell counter (Beckman Coulter, Fullerton, CA) up to 5 days. Each experiment was performed in duplicate sets at least twice.

Establishment of 14-3-3ζ-overexpressing HaCaT strains

The 14-3-3ζ-HA fragment from plasmid pcDNA3-14-3-3ζ-HA (Bialkowska et al., 2003) was excised by BamHI and EcoRI, and then cloned into pBABE retroviral vector. The pBABE-14-3-3ζ-HA plasmid was transfected into 40-50% confluent Phoenix packaging cells with Superfect transfection reagent (Qiagen) for 4 hours, then replaced with 10% FBS DMEM. After 48-hour incubation, the

supernatant was collected and placed on 40-50% confluent HaCaT cells in the presence of 8μg/ml polybrene for 48 hours. Transfected cells were selected with 2μg/ml puromycin.

Flow cytometry and BrdU-incorporation assay

Flow cytometry was used to determine DNA content of cells in exponential phase (propidium iodine, PI) and the rate of DNA synthesis by BrdU (5'-bromo-2'-deoxyuridine)-incorporation assay. Ethanol-fixed cells were treated with 200μg/ml RNAse A at 37°C and stained with 20μg/ml PI. As for BrdU- incorporation assay, we followed the manufacturer's FITC-BrdU Cell Proliferation Kit manual (BD Bioscience Pharmingen, San Diego CA). Cells were incubated with 10μM BrdU for 30 minutes, then harvested, permeabilized and fixed by provided reagents. 300μg/ml DNase I is used to nick genomic DNA for mouse FITC-conjugated anti-BrdU antibody to recognize. PI- or FITC-stained cells were analyzed with Beckman-Coulter flow cytometer and ModFit LT software (Verity Software House, Topsham, ME).

Results

RLGS and FISH analysis indicates gains on 14-3-3ζ copies

Our previous analysis identified RLGS fragment 2C13 on chromosome 8q22.3 as an amplified sequence in 14 out of 41 (~35%) tumor tissues in comparison to their normal counterparts (Lin et al., 2006). Chromosome 8q22.3 represents an independent amplicon in HNSCC, breast and prostate cancers and is located next the amplicon on 8q24.21, including the MYC oncogene (Chin et al., 2007; Garnis et al., 2004a; Saramaki et al., 2006). RLGS fragment 3D05, the neighboring fragment to 2C13, displays a similar frequency of enhancement and was co-amplified with 2C13 in the majority of cases. Both fragments reside within the 5' region of 14-3-3ζ, a tyrosine 3 / tryptophan 5-monooxygenase (Supplemental Figure S1). Here we used FISH analysis to examine and confirm the status of DNA amplification (Figure 1A, Table 1). Out of 48 patients, 33 had polysomy 8. 13 had low-level (14-3-3ζ/CEP8 = 2~4) and 3 had intermediate-level of copy number gain (14-3-3ζ/CEP8 = 4~10). No case of high-level copy number gain (ratio >10) was found. For comparison, the MYC locus on 8q24.21 showed low-level copy number gain in 10 patients, intermediate-level level of copy number gain in 5 and high-level level copy number gain (MYC/CEP8 > 20) in 1 case (data not shown). Overall, 33% (16/48) of the tumor samples carried extra 14-3-3ζ gene copies, which was comparable to the percentage determined by RLGS analysis. Results from both RLGS and FISH analyses indicated that gain of the 14-3-3ζ locus accounted for 30-40% HNSCC cases.

14-3-3ζ mRNA and protein are up-regulated in HNSCC patient samples

We used a second independent panel of HNSCC tissue samples to verify

elevated 14-3-3ζ mRNA levels by semi-quantitative RT-PCR (Figure 1B). 14-3-3ζ expression in 23 out of 44 tumor tissues was up-regulated (at least 2 fold over basal level) comparing to only 3 out of 41 normal tissues (p-value = 0.0024). Sub-categorization by tumor locations showed that 14-3-3ζ mRNA levels were more than 2-fold higher in 14 out of 17 tongue, 6 out of 8 oral cavity tumors, but only 3 out of 10 pharyngeal and none out of 9 laryngeal tumors. This data is conclusive with previous reports on elevated 14-3-3ζ mRNA levels in HNSCC (Matta et al., 2007).

To evaluate 14-3-3ζ protein levels, the same TMA set used in the FISH analysis was stained with an anti-14-3-3ζ antibody (Figure 1C). 14-3-3ζ protein staining was ubiquitous and stronger in tumors than in normal tissues. Some hyperplasic cells in normal tissues were also positive for 14-3-3ζ. Interestingly, in tumor sample PT91, whose 14-3-3ζ copy number gain was confirmed by FISH, there was no difference in 14-3-3ζ staining intensity between normal and tumor samples. A total of 37 out of 48 (77%) patients' tumor samples showed overexpression (Table 1). After further categorization, 8 cases had neither copy number gain nor overexpression, 3 had copy number gain but no overexpression, 24 had overexpression but no copy number gain and 13 had both copy number gain and overexpression. This data suggests that cancer cells can overexpress 14-3-3ζ protein frequently through mechanisms other than copy number gains.

Down- and up-regulation of 14-3-3ζ greatly affects cell growth

The effects by temporary knockdown of 14-3-3ζ by RNAi were examined in three HNSCC (UMSCC-8, -11B and -22B) and HaCaT cell lines (Figure 2A). 14-3-3ζ RNAi successfully reduced the amount of its protein in all four tested

cell lines in various degrees. Our RNAi sequence of choice reduced 14-3-3ζ levels greatly in UMSCC-8 and UMSCC-22B, but mildly on UMSCC-11B and HaCaT, approximately to 0.5 fold compared to their original levels in those cell lines. In UMSCC-22B line, the 14-3-3ζ RNAi was able to inhibit the protein level for at least 4 days, more than the time needed for short-term experiments (Figure 2B). In a 5-day interval, 14-3-3ζ RNAi also greatly suppressed the cell population in all three tested cell lines, even in UMSCC-11B and HaCaT cells, which still had ~0.5 fold of original 14-3-3ζ levels (Figure 2C).

We also established the non-cancerous HaCaT cell line with ectopically-transfected 14-3-3ζ. Although HaCaT, along with all tested HNSCC cell lines, already had abundant endogenous 14-3-3ζ protein, our 14-3-3ζ-transfected HaCaT cells expressed twice the amount of vector-transfected control (Figure 3A). HaCaT cells with nearly doubled 14-3-3ζ level attained a population density nearly twice that of vector control after 5 days (Figure 3B). There was no immediate morphological change between normal and 14-3-3ζ-reduced HaCaT cells after 10 passages (p10) following the initial transfection (Figure 3C, top row). However, 10 passages later (p20), we observed that all 14-3-3ζ-overexpressing cells underwent morphological changes, from flatter original HaCaT cells to spinde-shaped cells (Figure 3C, middle and bottom rows). These cells were also highly clustered, possibly due to rapid proliferation. They were more easily detached by trypsin during passages than original HaCaT cells. Western blotting revealed decreased levels of E-cadherin and expression of vimentin, supporting that these cells have undergone epithelial-mesenchymal transition (EMT), which is considered a step closer toward metastasis (Figure 3D). These experiments demonstrated that inhibition and overexpression of

14-3-3ζ have immediate and profound impacts on cell growth and morphology.

14-3-3ζ inhibition affects cell cycle and DNA synthesis

Based on results from the inhibition and overexpression experiments, we wanted to determine whether 14-3-3ζ regulates cell populations by accelerating cell cycle progression or blocking apoptosis. Flow cytometry was used to address this question. For DNA content index, cells were treated with 60 nM scrambled RNAi or 14-3-3ζ RNAi for 3 days before being fixed and stained by PI. H1299 lung adenocarcinoma cell line was used as a control (Neal, 2004). Figure 4A showed that 14-3-3ζ RNAi reduced the proportion of S phase and increases that of G1/G0 phase in both HaCaT and H1299 cell lines. No change in either sub-G1 (apoptotic body) or G2/M proportion was detected after 14-3-3ζ RNAi treatment. Next we used the BrdU-incorporation assay to determine the proportion of cells entering S-phase. Both HaCaT and H1299 cells transfected with 14-3-3ζ RNAi incorporate less BrdU than their negative controls (Figure 4B). However, both DNA content index and BrdU-incorporation assay were unable to detect any differences between original and 14-3-3ζ-overexpressing HaCaT cells (data not shown). These findings supported that 14-3-3ζ regulates cell population by accelerating cell cycle progression instead of blocking apoptosis.

Discussion

In this study we showed that chromosome 8q22.3 gain is seen in 30-40% of HNSCC patients. 30-40% is a significant number in HNSCC, for that three other major amplicons (3q26.3, 8q24.21 and 11q13.3) all had similar incidences of amplification with three major proven oncogenes (PIK3CA, MYC and CCND1) located in them, respectively (Lin et al., 2006). Frequent amplification of a specific gene may imply its importance in carcinogenesis, since the cells are inclined to keep it during natural cycles of proliferation and death. It also implies that 14-3-3ζ might be an initiator in the early stage of carcinogenesis instead of merely a downstream effector, which is unlikely to be selectively amplified and kept in such a high rate. This hypothesis is supported by the alternative pathological and statistical approaches (Matta et al., 2007). We have seen the oncogenic potentials of PIK3CA, MYC and CCND1 in cancers including HNSCC, and our study suggests that 14-3-3ζ should be an additional major gene to study in HNSCC carcinogenesis.

In addition to 14-3-3ζ, there are other genes which are amplified and overexpressed in the proximity of 8q22.3 in HNSCC, thus there is a possibility that 14-3-3ζ is not the only proto-oncogene in this chromosomal region as described also for other chromosomal amplifications (Freier et al., 2006). Gene EDD, the human orthologue of the hyperplastic discs tumor suppressor gene, is amplified and overexpressed in multiple cancers (Clancy et al., 2003). EDD is only ~1.3 Mbp away from 14-3-3ζ. Another amplified and overexpressed gene LRP12 is ~3.5 Mb away (Garnis et al., 2004b). BAALC (brain and acute leukemia, cytoplasmic, ~2.2 Mb away) is found to be associated with acute myeloid leukemia (AML) (Baldus et al., 2003). There are no reports of characterization of their oncogenic potentials. On the other hand,

14-3-3 family is known to be involved in signal transduction, which is one of the major reasons we studied it first, along with its extreme proximity to our RLGS fragments. Whether other genes are merely co-amplified with 14-3-3ζ or they possess oncogenic potentials remain unanswered.

One of the important characteristics for 14-3-3ζ is the ability to promote cell growth when overexpressed in this study. However, overexpression of some proven oncogenes more likely leads cells to senescence rather than outgrowth. Hyperactive Ras (RasV12) and c-Myc-induced senescence in human or mouse fibroblasts is well documented and a powerful tool to study other oncogenes (Di Micco et al., 2006; Felsher et al., 2000; Grandori et al., 2003). Mounting evidence shows that whenever an oncogene is overrepresented, many cell cycle inhibitors will be activated and block further cell cycle progression, which is regarded as the intrinsic defense mechanism. Cells remain arrested until a second defect such as p53 mutation switches off these defenses, then transform (Mallette & Ferbeyre, 2007). Overexpressing 14-3-3ζ is capable of transforming immortalized mouse fibroblasts NIH3T3 when co-transfected with RasV12 (Neal, 2004). It is possible that HaCaT may have possessed needed components to allow 14-3-3ζ to promote growth.

The growth-promoting activity of 14-3-3ζ has been demonstrated *in vitro*, but we did not address its effects on apoptosis. The idea of 14-3-3ζ being anti-apoptotic is supported in many reports. 14-3-3ζ binds to Bad of the pro-apoptotic BCL2 family member (Yang et al., 2001). High-level 14-3-3ζ is known to protect cells from insults such as anti-tumor agents, radiation and anoikis (Fan et al., 2007; Li et al., 2008; Qi & Martinez, 2003). Based on our growth experiments, cells with reduced 14-3-3ζ level proliferated less not due to inducing apoptosis since the sub-G1 proportion was neglectable. Inhibiting

14-3-3ζ level is likely to increase cells' susceptibility to anti-tumor agents and insults, but for 14-3-3ζ to regulate cell growth, functional apoptotic machinery may not be required.

Interestingly, a unpublished study observed that transgenic mice with extra 14-3-3ζ gene copies developed various types of tumors by the age of 7-15 months in about 15% of the animals (Tzivion et al., 2006). Here the level of expression of 14-3-3ζ in transgenic mice was only 30% greater than that in normal ones. This observation corroborates very well with our observations: (1) 14-3-3ζ copy number gain was only 2-4 fold in HNSCC patients; (2) knocking out merely a half of 14-3-3ζ production in HaCaT was sufficient to suppress its growth; (3) merely doubling 14-3-3ζ level was able to promote HaCaT growth and in a long term, induce morphological changes and EMT. It may only need low-level amplification or expression for 14-3-3ζ gene to exert it effects toward cell transformation.

Acknowledgements

We thank Dr. Thomas Carey, University of Michigan for HNSCC cell lines UMSCC-8, -9, -11B and -22B, Dr. Andrzej Slominski, University of Tennessee Health Science Center for HaCaT cells, plasmid pCDNA3-14-3-3ζ-HA was a kind gift from Dr. Joan E.B. Fox, Case Western Reserve University (originally designed by Dr. Charles Adams, University of Pennsylvania) and pBABE retroviral vector was provided by Dr. Gokhan Hotamisligil, Harvard University. This work was supported by NIH grant ROI 13123 (CP).

Reference

Aitken, A., Howell, S., Jones, D., Madrazo, J. & Patel, Y. (1995). *J Biol Chem*, **270,** 5706-9.

Arora, S., Matta, A., Shukla, N.K., Deo, S.V. & Ralhan, R. (2005). *Mol Carcinog*, **42,** 97-108.

Baldus, C.D., Tanner, S.M., Ruppert, A.S., Whitman, S.P., Archer, K.J., Marcucci, G., Caligiuri, M.A., Carroll, A.J., Vardiman, J.W., Powell, B.L., Allen, S.L., Moore, J.O., Larson, R.A., Kolitz, J.E., de la Chapelle, A. & Bloomfield, C.D. (2003). *Blood*, **102,** 1613-8.

Bialkowska, K., Zaffran, Y., Meyer, S.C. & Fox, J.E. (2003). *The Journal of biological chemistry*, **278,** 33342-50.

Bitzer, M., Stahl, M., Arjumand, J., Rees, M., Klump, B., Heep, H., Gabbert, H.E. & Sarbia, M. (2003). *Anticancer Res*, **23,** 1489-93.

Braselmann, S. & McCormick, F. (1995). *Embo J*, **14,** 4839-48.

Chin, S.F., Teschendorff, A.E., Marioni, J.C., Wang, Y., Barbosa-Morais, N.L., Thorne, N.P., Costa, J.L., Pinder, S.E., van de Wiel, M.A., Green, A.R., Ellis, I.O., Porter, P.L., Tavare, S., Brenton, J.D., Ylstra, B. & Caldas, C. (2007). *Genome biology*, **8,** R215.

Clancy, J.L., Henderson, M.J., Russell, A.J., Anderson, D.W., Bova, R.J., Campbell, I.G., Choong, D.Y., Macdonald, G.A., Mann, G.J., Nolan, T., Brady, G., Olopade, O.I., Woollatt, E., Davies, M.J., Segara, D., Hacker, N.F., Henshall, S.M., Sutherland, R.L. & Watts, C.K. (2003). *Oncogene*, **22,** 5070-81.

Di Micco, R., Fumagalli, M., Cicalese, A., Piccinin, S., Gasparini, P., Luise, C., Schurra, C., Garre, M., Nuciforo, P.G., Bensimon, A., Maestro, R., Pelicci, P.G. & d'Adda di Fagagna, F. (2006). *Nature*, **444,** 638-42.

Fan, T., Li, R., Todd, N.W., Qiu, Q., Fang, H.B., Wang, H., Shen, J., Zhao, R.Y., Caraway, N.P., Katz, R.L., Stass, S.A. & Jiang, F. (2007). *Cancer research*, **67,** 7901-6.

Felsher, D.W., Zetterberg, A., Zhu, J., Tlsty, T. & Bishop, J.M. (2000). *Proceedings of the National Academy of Sciences of the United States of America*, **97,** 10544-8.

Freier, K., Sticht, C., Hofele, C., Flechtenmacher, C., Stange, D., Puccio, L., Toedt, G., Radlwimmer, B., Lichter, P. & Joos, S. (2006). *Genes, chromosomes & cancer*, **45,** 118-25.

Gallegos Ruiz, M.I., Floor, K., Vos, W., Grunberg, K., Meijer, G.A., Rodriguez, J.A. & Giaccone, G. (2007). *Histopathology*, **51,** 631-7.

Garnis, C., Coe, B.P., Ishkanian, A., Zhang, L., Rosin, M.P. & Lam, W.L.

(2004a). *Genes, chromosomes & cancer*, **39,** 93-8.
Garnis, C., Coe, B.P., Zhang, L., Rosin, M.P. & Lam, W.L. (2004b). *Oncogene*, **23,** 2582-6.
Grandori, C., Wu, K.J., Fernandez, P., Ngouenet, C., Grim, J., Clurman, B.E., Moser, M.J., Oshima, J., Russell, D.W., Swisshelm, K., Frank, S., Amati, B., Dalla-Favera, R. & Monnat, R.J., Jr. (2003). *Genes & development*, **17,** 1569-74.
Green, A.J. (2002). *Neuropathol Appl Neurobiol*, **28,** 427-40.
Jang, J.S., Cho, H.Y., Lee, Y.J., Ha, W.S. & Kim, H.W. (2004). *Oncol Res*, **14,** 491-9.
Jones, D.H., Ley, S. & Aitken, A. (1995). *FEBS Lett*, **368,** 55-8.
Laronga, C., Yang, H.Y., Neal, C. & Lee, M.H. (2000). *J Biol Chem*, **275,** 23106-12.
Lee, M.H. & Lozano, G. (2006). *Semin Cancer Biol*, **16,** 225-34.
Li, R., Wang, H., Bekele, B.N., Yin, Z., Caraway, N.P., Katz, R.L., Stass, S.A. & Jiang, F. (2006). *Oncogene*, **25,** 2628-35.
Li, Z., Zhao, J., Du, Y., Park, H.R., Sun, S.Y., Bernal-Mizrachi, L., Aitken, A., Khuri, F.R. & Fu, H. (2008). *Proceedings of the National Academy of Sciences of the United States of America*, **105,** 162-7.
Lin, M., Smith, L.T., Smiraglia, D.J., Kazhiyur-Mannar, R., Lang, J.C., Schuller, D.E., Kornacker, K., Wenger, R. & Plass, C. (2006). *Oncogene*, **25,** 1424-33.
Lyons, S.K. & Clarke, A.R. (1997). *Br Med Bull*, **53,** 554-69.
Mallette, F.A. & Ferbeyre, G. (2007). *Cell cycle (Georgetown, Tex*, **6,** 1831-6.
Matta, A., Bahadur, S., Duggal, R., Gupta, S.D. & Ralhan, R. (2007). *BMC cancer*, **7,** 169.
Moore, B.W. & Perez, V.J. *Specific Acid Proteins in Nervous System*. Prentice-Hall: Englewood Cliffs, N. J.,.
Morrison, C., Radmacher, M., Mohammed, N., Suster, D., Auer, H., Jones, S., Riggenbach, J., Kelbick, N., Bos, G. & Mayerson, J. (2005). *Journal of clinical oncology*, **23,** 9369-76.
Muller, W.E., Laplanche, J.L., Ushijima, H. & Schroder, H.C. (2000). *Mech Ageing Dev*, **116,** 193-218.
Neal, C.L. (2004). *Graduate School of Biomedical Sciences*. University of Texas: Houston, Texas, pp 190.
Neve, R.M., Lane, H.A. & Hynes, N.E. (2001). *Ann Oncol*, **12 Suppl 1,** S9-13.
Nomura, M., Shimizu, S., Sugiyama, T., Narita, M., Ito, T., Matsuda, H. & Tsujimoto, Y. (2003). *J Biol Chem*, **278,** 2058-65.
Okada, T., Masuda, N., Fukai, Y., Shimura, T., Nishida, Y., Hosouchi, Y.,

Kashiwabara, K., Nakajima, T. & Kuwano, H. (2006). *Anticancer Res*, **26,** 3105-10.
Perathoner, A., Pirkebner, D., Brandacher, G., Spizzo, G., Stadlmann, S., Obrist, P., Margreiter, R. & Amberger, A. (2005). *Clin Cancer Res*, **11,** 3274-9.
Qi, W. & Martinez, J.D. (2003). *Radiation research*, **160,** 217-23.
Ralhan, R., Desouza, L.V., Matta, A., Chandra Tripathi, S., Ghanny, S., Datta Gupta, S., Bahadur, S. & Siu, K.W. (2008). *Molecular & cellular proteomics*, **7,** 1162-73.
Richard, M., Biacabe, A.G., Streichenberger, N., Ironside, J.W., Mohr, M., Kopp, N. & Perret-Liaudet, A. (2003). *Acta Neuropathol (Berl)*, **105,** 296-302.
Rittinger, K., Budman, J., Xu, J., Volinia, S., Cantley, L.C., Smerdon, S.J., Gamblin, S.J. & Yaffe, M.B. (1999). *Mol Cell*, **4,** 153-66.
Robinson, K., Jones, D., Patel, Y., Martin, H., Madrazo, J., Martin, S., Howell, S., Elmore, M., Finnen, M.J. & Aitken, A. (1994). *Biochem J*, **299 (Pt 3),** 853-61.
Saramaki, O.R., Porkka, K.P., Vessella, R.L. & Visakorpi, T. (2006). *International journal of cancer*, **119,** 1322-9.
Schwab, M. (1999). *Semin Cancer Biol*, **9,** 319-25.
Schwab, M. & Amler, L.C. (1990). *Genes Chromosomes Cancer*, **1,** 181-93.
Tian, Q., Feetham, M.C., Tao, W.A., He, X.C., Li, L., Aebersold, R. & Hood, L. (2004). *Proc Natl Acad Sci U S A*, **101,** 15370-5.
Tzivion, G., Gupta, V.S., Kaplun, L. & Balan, V. (2006). *Seminars in cancer biology*, **16,** 203-13.
Villaret, D.B., Wang, T., Dillon, D., Xu, J., Sivam, D., Cheever, M.A. & Reed, S.G. (2000). *Laryngoscope*, **110,** 374-81.
Yaffe, M.B., Rittinger, K., Volinia, S., Caron, P.R., Aitken, A., Leffers, H., Gamblin, S.J., Smerdon, S.J. & Cantley, L.C. (1997). *Cell*, **91,** 961-71.
Yang, H., Masters, S.C., Wang, H. & Fu, H. (2001). *Biochimica et biophysica acta*, **1547,** 313-9.
Yang, H.Y., Wen, Y.Y., Chen, C.H., Lozano, G. & Lee, M.H. (2003). *Mol Cell Biol*, **23,** 7096-107.

Figure Legends

Figure 1. 14-3-3ζ copy number gain, mRNA and protein overexpression in HNSCC.

A. Low-level copy number gain of 14-3-3ζ gene by FISH. The red signals are BAC clone RP11-302J23 to detect 14-3-3ζ gene copies. The green signals are CEP8 probe to detect centromeres of chromosome 8 as the internal control.

B. mRNA levels in HNSCC patients' normal and tumor samples. Red line indicates two folds and green line indicates 0.5 fold. 14-3-3ζ mRNA levels of 34 out of 41 normal samples and 16 out of 44 tumors fall between 0.5 to 2 folds.

C. Immunohistochemistry of 14-3-3ζ protein in four pairs of normal and tumor samples. 14-3-3ζ protein is stained brown. Magnification is 100X.

Figure 2. 14-3-3ζ RNAi inhibits cell population.

A. Western blotting of 14-3-3ζ protein after 3-day treatment of scrambled (-) or 14-3-3ζ (+) RNAi (both 60nM). α-tubulin serves as the internal control. 14-3-3ζ RNAi reduces target protein levels in all four cell lines.

B. Time course of the inhibitory effect of 14-3-3ζ RNAi in UMSCC-22B cell line. 14-3-3ζ RNAi suppresses protein levels for at least four days.

C. Growth curve of three cell lines under 14-3-3ζ RNAi. 14-3-3ζ RNAi suppresses cell growth in all cell lines (starting 20K cells, 5-days interval).

Figure 3. 14-3-3ζ overexpression in human keratinocyte line causes cell overgrowth and morphological changes.

A. Western blotting confirms HA-tagged 14-3-3ζ ectopic overexpression in stable-transfected HaCaT cell line in spite of a high endogenous 14-3-3ζ level.

B. Growth curve of 14-3-3ζ-HA-transfected HaCaT line. It shows more rapid growth than negative vector control line in regular 10% FBS DMEM.

C. HaCaT cell growth and morphology. Top row, left to right: HaCaT cells with vector only (passage 10) and with overexpressed 14-3-3ζ-HA (passage 10). Middle row, left to right: HaCaT cells with vector only (passage 20) and with 14-3-3ζ (passage 20). 100X magnification. Bottom row, 400X magnification.

D. Western blotting of EMT markers (E-cadherin, vimentin) in vector control and 14-3-3ζ-overexpressing HaCaT cells. Full length of E-cadherin is 120KDa. 80KDa fragment is the proteolytic product.

Figure 4. 14-3-3ζ RNAi affects cell cycle and DNA synthesis.

A. DNA content in H1299 and HaCaT cells treated with scrambled RNAi or 14-3-3ζ RNAi. The left peak represents the G0/G1 phase and the right peak represents the G2/M phase. S phase is between these two peaks. Percentage of each phase is calculated by ModFit LT software.

B. BrdU-incorporation assay in H1299 and HaCaT cells. The number represents the percentage of the BrdU-positive (S-phase) cells in each population. Each set is done in duplicate.

Table Legends

Table 1. Summary of FISH analysis and immunohistochemistry for 14-3-3ζ gene copy and protein level in HNSCC

Polysomy 8 is highlighted in yellow color in Polysomy 8 column. Yellow color in 14-3-3ζ/CEP column as low level of amplification and orange as intermediate level. Symbols in IHC expression column: +++, high level; ++, intermediate level; +, low level; -, no staining.

Supplemental Materials

Figure S1. The structure and location of 14-3-3ζ on chromosome 8q22.3. The figure is the remake of the result from UCSC bioinfomatic website search. The top row of numbers indicates the actual base pair. The YWHAZ/14-3-3ζ gene is laid out as the bottom line consisted of blue boxes (exons) and arrowheads (orientation). Fragment 2C13 and 3D05 are colored as red and green boxes, respectively.

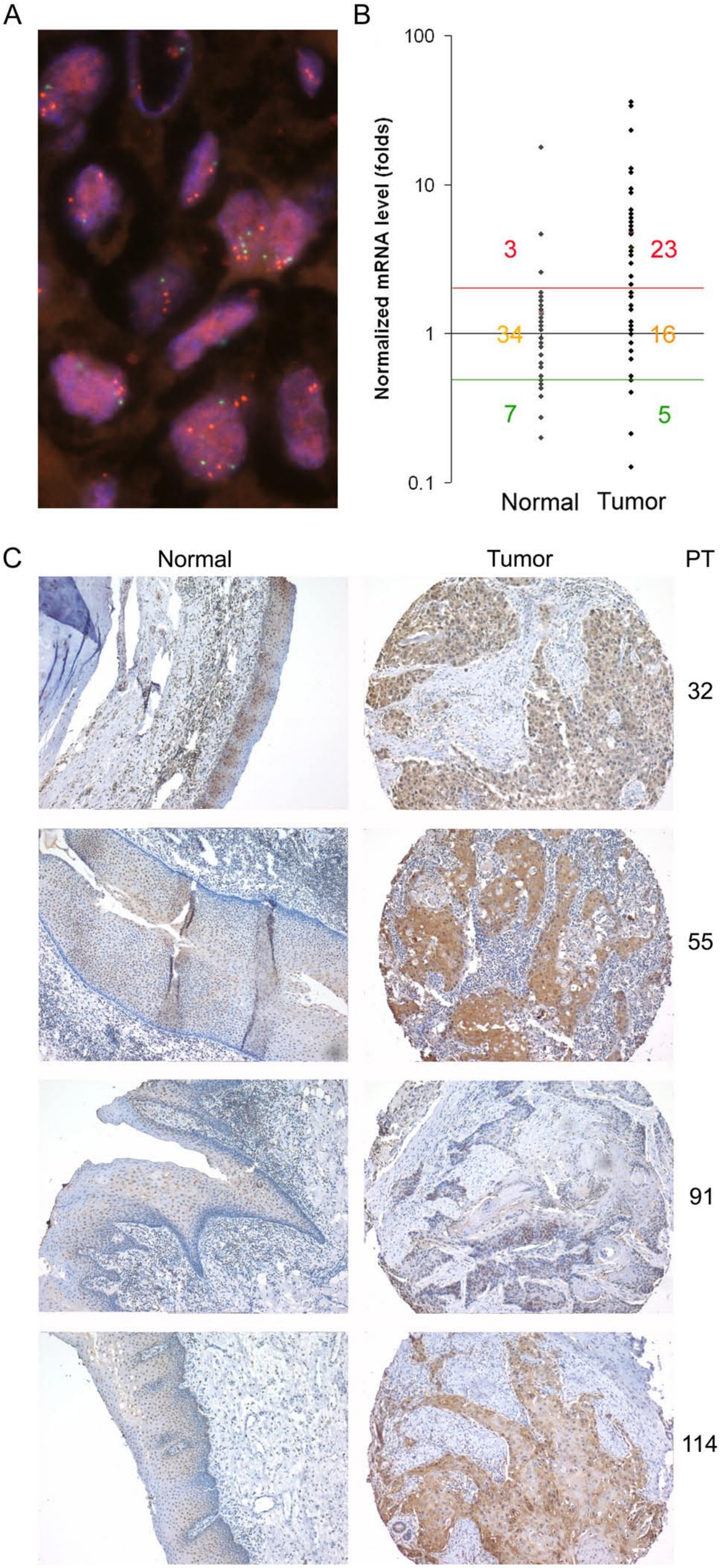
A
B
100
10
1
0.1
Normalized mRNA level (folds)
3
23
34
16
7
5
Normal
Tumor
C
Normal
Tumor
PT
32
55
91
114

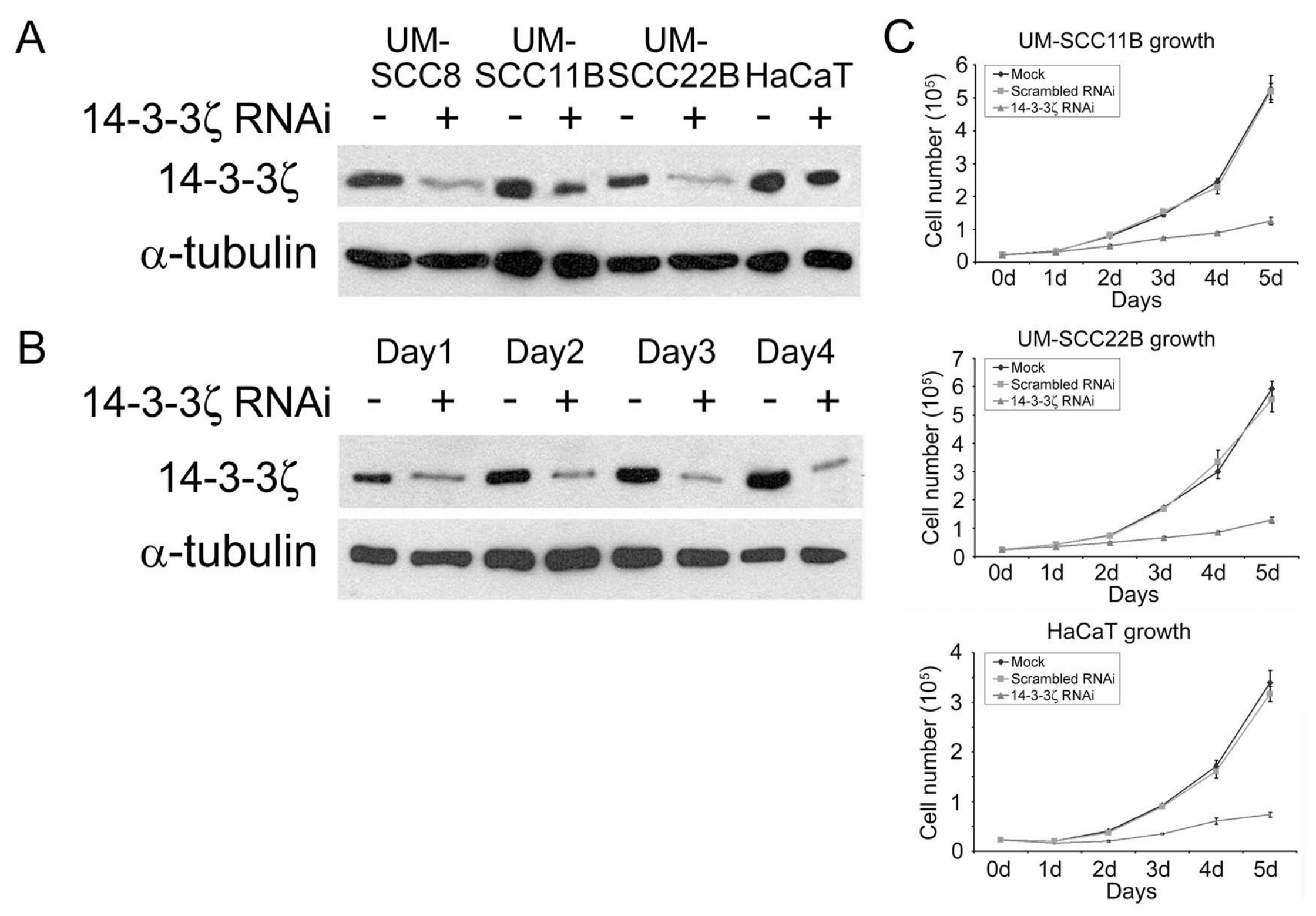
A
UM-SCC8
UM-SCC11B
UM-SCC22B
HaCaT
14-3-3ζ RNAi
- + - + - + - +
14-3-3ζ
α-tubulin
B
Day1
Day2
Day3
Day4
14-3-3ζ RNAi
- + - + - + - +
14-3-3ζ
α-tubulin
C
UM-SCC11B growth
Mock
Scrambled RNAi
14-3-3ζ RNAi
Cell number (10^5)
0 1 2 3 4 5 6
0d 1d 2d 3d 4d 5d
Days
UM-SCC22B growth
Mock
Scrambled RNAi
14-3-3ζ RNAi
Cell number (10^5)
0 1 2 3 4 5 6 7
0d 1d 2d 3d 4d 5d
Days
HaCaT growth
Mock
Scrambled RNAi
14-3-3ζ RNAi
Cell number (10^5)
0 1 2 3 4
0d 1d 2d 3d 4d 5d
Days

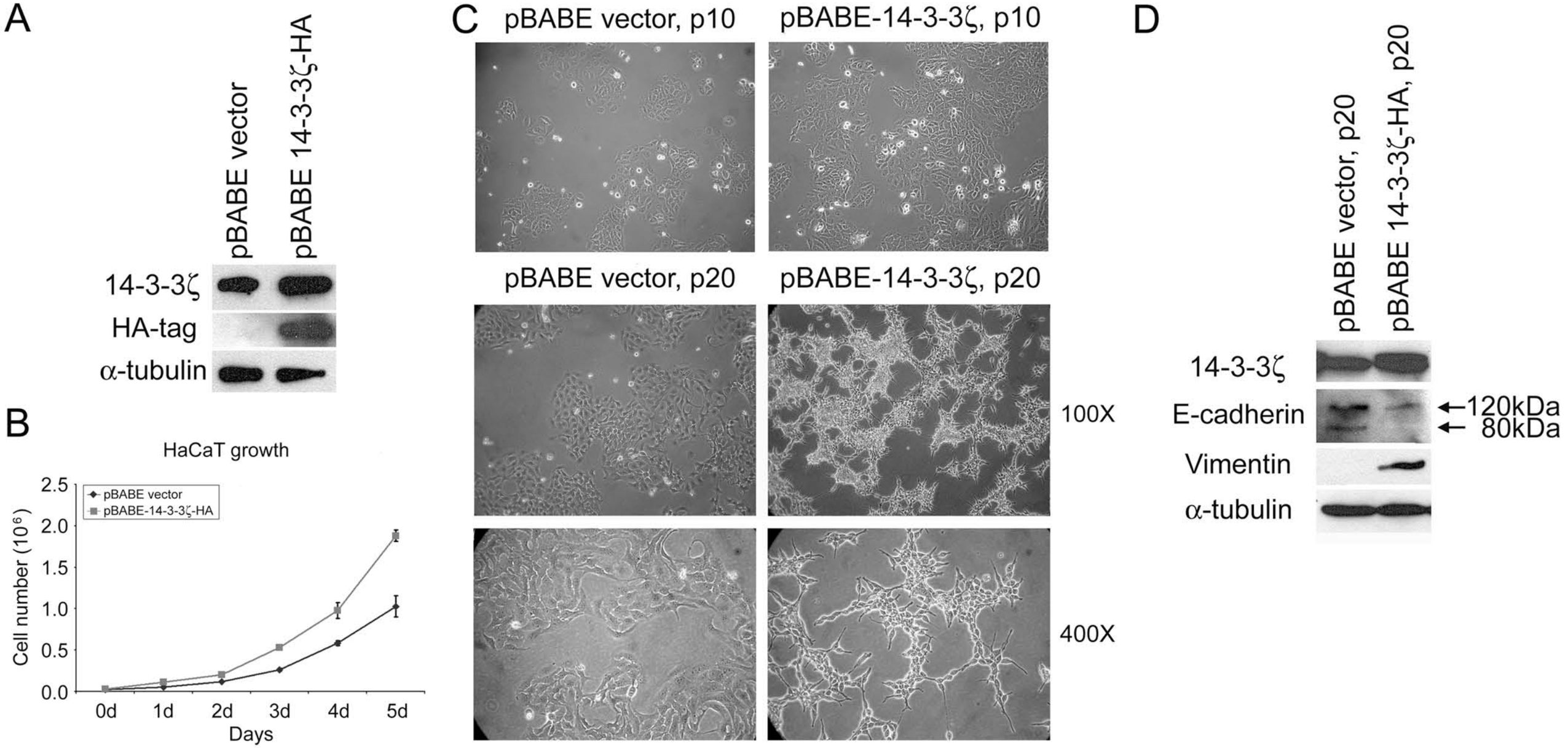
A
pBABE vector
pBABE 14-3-3ζ-HA
14-3-3ζ
HA-tag
α-tubulin
B
HaCaT growth
pBABE vector
pBABE-14-3-3ζ-HA
Cell number (10^6)
2.5
2.0
1.5
1.0
0.5
0.0
0d
1d
2d
3d
4d
5d
Days
C
pBABE vector, p10
pBABE-14-3-3ζ, p10
pBABE vector, p20
pBABE-14-3-3ζ, p20
100X
400X
D
pBABE vector, p20
pBABE 14-3-3ζ-HA, p20
14-3-3ζ
E-cadherin
120kDa
80kDa
Vimentin
α-tubulin

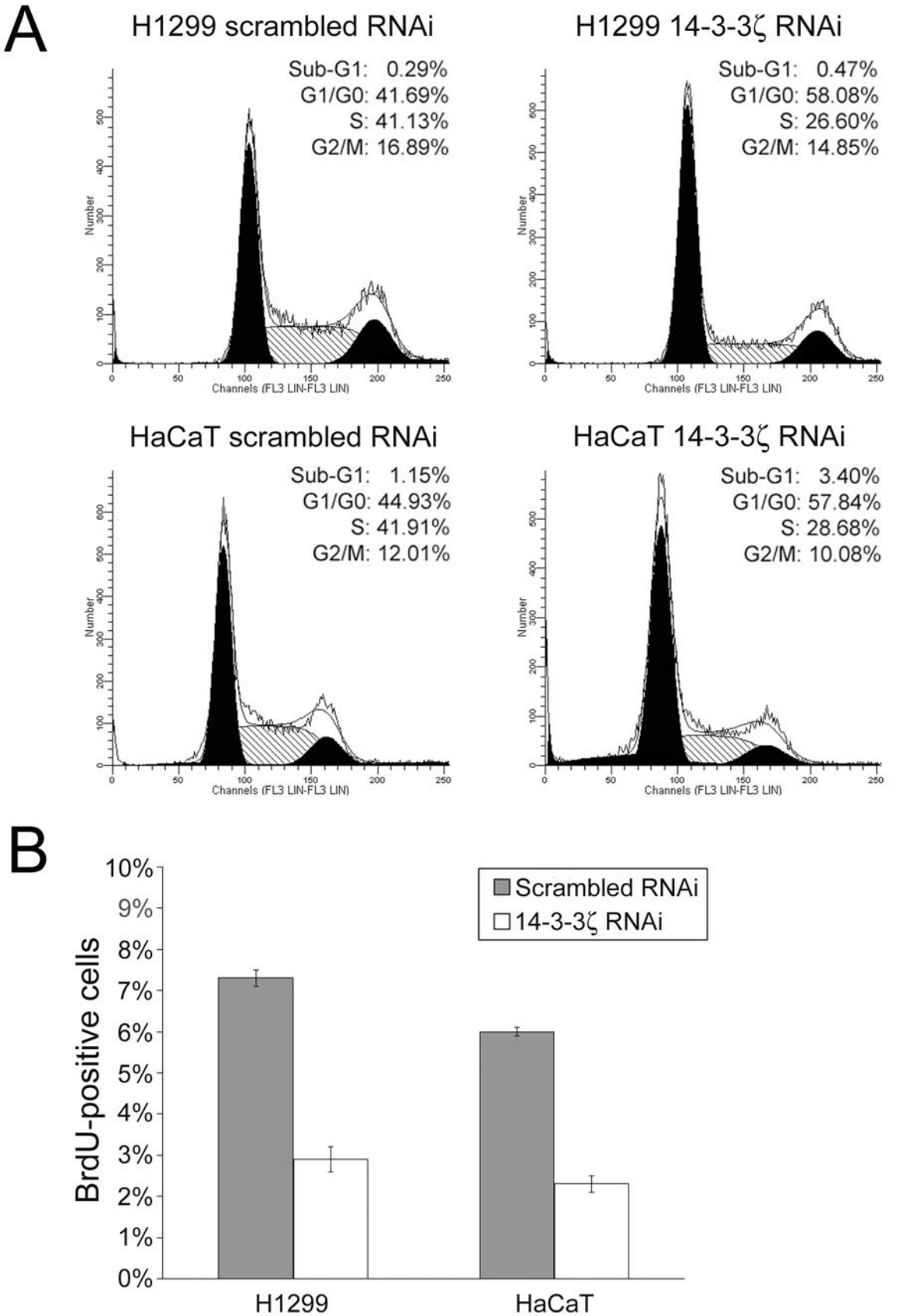
A
H1299 scrambled RNAi
Sub-G1: 0.29%
G1/G0: 41.69%
S: 41.13%
G2/M: 16.89%
H1299 14-3-3ζ RNAi
Sub-G1: 0.47%
G1/G0: 58.08%
S: 26.60%
G2/M: 14.85%
HaCaT scrambled RNAi
Sub-G1: 1.15%
G1/G0: 44.93%
S: 41.91%
G2/M: 12.01%
HaCaT 14-3-3ζ RNAi
Sub-G1: 3.40%
G1/G0: 57.84%
S: 28.68%
G2/M: 10.08%
Number
Channels (FL3 LIN-FL3 LIN)
B
BrdU-positive cells
10%
9%
8%
7%
6%
5%
4%
3%
2%
1%
0%
Scrambled RNAi
14-3-3ζ RNAi
H1299
HaCaT

PHNT ID	Polysomy 8	RP11-302J23 (14-3-3ζ)/CEP8	14-3-3ζ amplification status	Expression level
4	yes	3.56	Low level	+++
7	no	<1.8	No amplification or deletion	++
8	yes	<1.8	No amplification or deletion	+++
11	yes	1.95	Indeterminate	+
12	yes	<1.8	No amplification or deletion	+++
13	yes	<1.8	No amplification or deletion	+++
14	yes	<1.8	No amplification or deletion	++
15	no	<1.8	No amplification or deletion	-
22	yes	<1.8	No amplification or deletion	++
23	no	<1.8	No amplification or deletion	-
24	no	2.35	Low level	++
25	no	5.94	Intermediate level	+++
27	yes	<1.8	No amplification or deletion	++
28	no	<1.8	No amplification or deletion	++
29	yes	2.41	Low level	+++
32	yes	<1.8	No amplification or deletion	+++
39	no	<1.8	No amplification or deletion	+
40	yes	<1.8	No amplification or deletion	+++
46	no	3.1	Low level	-
47	yes	2.41	Low level	++
49	yes	<1.8	No amplification or deletion	+++
50	yes	2.89	Low level	+++
54	yes	5.87	Intermediate level	+
55	yes	4.59	Intermediate level	+++
56	yes	3.84	Low level	++
71	no	<1.8	No amplification or deletion	+++
82	yes	2.89	Low level	+
91	yes	<1.8	No amplification or deletion	-
99	yes	<1.8	No amplification or deletion	-
106	yes	<1.8	No amplification or deletion	++
110	yes	<1.8	No amplification or deletion	-
114	yes	<1.8	No amplification or deletion	+++
115	no	<1.8	No amplification or deletion	+++
118	yes	3.05	Low level	++
126	yes	<1.8	No amplification or deletion	++

129	no	<1.8	No amplification or deletion	-
130	yes	2.25	Low level	+
132	no	<1.8	No amplification or deletion	+++
145	no	<1.8	No amplification or deletion	-
158	yes	2.56	Low level	-
159	yes	<1.8	No amplification or deletion	+
167	yes	<1.8	No amplification or deletion	+++
173	no	2.04	Indeterminate	-
180	yes	2.06	Indeterminate	+
192	yes	<1.8	No amplification or deletion	++
193	no	3.22	Low level	-
201	yes	2.15	Indeterminate	+
220	yes	3.41	Low level	+++